Within-host dynamics explain the coexistence of antibiotic-sensitive and resistant bacteria

Nicholas G. Davies[1,2], *Stefan Flasche*[1,2], *Mark Jit*[1,2,3], *Katherine E. Atkins*[1,2]

[1]Centre for Mathematical Modelling of Infectious Diseases, London School of Hygiene and Tropical Medicine, London, UK

[2]Department for Infectious Disease Epidemiology, Faculty of Epidemiology and Population Health, London School of Hygiene and Tropical Medicine, London, UK

[3]Modelling and Economics Unit, Public Health England, London, UK

Corresponding Author: Nicholas.Davies@lshtm.ac.uk

Antibiotic resistance is one of the foremost threats to human health[1,2], yet the spread of resistance is poorly understood. Resistant and sensitive strains of the same bacteria nearly always coexist in host populations[3–5], but mathematical models of disease transmission have failed to identify a general, empirically-supported mechanism that can reproduce this phenomenon[6–9]. Such a model should be structurally neutral[10], meaning that coexistence arises from the biology of sensitive and resistant strains rather than being an assumption embedded into the model structure. However, existing models have only applied the principle of structural neutrality at the population level, not within individual hosts where resistant and sensitive strains may interact. Here, we show that within-host dynamics between resistant and sensitive strains creates frequency-dependent selection for resistance, promoting coexistence at the population level, and that extending structural neutrality to the within-host level allows us to reproduce empirical patterns of resistance in commensal bacteria across 30 European countries. In doing so, we identify a parsimonious and biologically-plausible explanation for coexistence that resolves a long-standing conflict between theoretical prediction and empirical observation. Simple mathematical models that mechanistically capture resistance transmission dynamics will allow us to more accurately predict the impact of much-needed strategies for managing resistance.

When two different species compete for the same resource, standard ecological theory predicts competitive exclusion: that the better-adapted species will fully outcompete the other[11]. If instead, long-term coexistence between competitors is

38 observed, then either the two species occupy different niches, or there is a
39 mechanism that specifically promotes species diversity[11]. One such mechanism is
40 negative frequency-dependent selection[12], in which an individual's fitness is
41 higher when their species is rarer. Negative frequency dependence has long been
42 known to promote stable coexistence among animal[13, 14], plant[15], and bacterial[16]
43 competitors. Here, we argue that it may also have a hitherto underappreciated
44 role in the spread of antibiotic resistance.
45
46 The simplest epidemiological model of antibiotic resistance assumes that hosts
47 can be colonised by either a sensitive or a resistant strain, but not both
48 simultaneously (**Fig. 1a**). In this single carriage model, sensitive strains benefit
49 from a fitness advantage in the absence of antibiotic treatment[17, 18], while
50 resistant strains benefit from being unaffected by antibiotics. Lacking any
51 selection for strain diversity, this model results in competitive exclusion, such
52 that above a particular threshold rate of treatment, resistant strains fully
53 outcompete sensitive strains, while below it, they are unable to emerge at all
54 (**Fig. 1b**). This competitive exclusion is not observed empirically, and there is
55 little evidence that the intermediate resistance prevalences we observe are only
56 transient states on the way to competitive exclusion[7]. Instead, sensitive and
57 resistant strains of the same bacteria stably coexist in natural populations[7–9],
58 with the prevalence of resistance to a particular antibiotic gradually increasing
59 with consumption of that antibiotic[3–5] (**Fig. 1c**). Existing mathematical models
60 are not in agreement over how best to explicitly integrate our biological and
61 epidemiological understanding into a general mechanism that reconciles our
62 theoretical understanding of antibiotic resistance with observed patterns of

63 coexistence. However, without a mechanistic understanding of resistance
64 dynamics, we cannot predict the likely impact of public health interventions for
65 managing resistance.
66
67 One way to resolve this discrepancy between theory and observation is to
68 introduce simultaneous dual carriage of both sensitive and resistant strains[7, 19].
69 Although dual carriage is known to promote coexistence[7], the mechanism by
70 which it does so has remained unclear. Here, we identify frequency-dependent
71 selection for resistance as the mechanism by which dual carriage promotes
72 coexistence. Specifically, if resistant cells are successfully transmitted to a host
73 already carrying a sensitive strain, and that host subsequently undergoes
74 antibiotic treatment, the resident sensitive strain is killed and the invading
75 resistant cells can grow in number to fully occupy the host niche (**Fig 1d**). By
76 contrast, if resistant cells are instead transmitted to a host already carrying a
77 resistant strain, subsequent treatment has no such effect. Hence, resistant strains
78 enjoy a relative fitness advantage when sensitive-strain carriers are more
79 common. As the resistant strain multiplies, sensitive-strain carriers become less
80 common, and this frequency-dependent advantage diminishes. Coexistence
81 stabilises at intermediate frequencies when the sensitive and resistant strains
82 have equal fitness.
83
84 To further investigate dual carriage as a mechanism for coexistence, we began by
85 analysing a parsimonious mathematical model of dual carriage[7, 19] in which there
86 is one class of non-carriers, X, and three classes of carriers: S carriers, who are
87 colonised by the sensitive strain; R carriers, who are colonised by the resistant

88 strain; and *SR* carriers, who are colonised by both strains in equal measure (**Fig.**
89 **2a**). In this model, dual carriage occurs when *S* or *R* carriers are colonised by the
90 strain they do not carry through contact with other single or dual carriers. If an
91 *SR* carrier is again re-colonised, "knockout" occurs, with the incoming strain
92 taking the place of one of the two resident strains: for example, an *SR* carrier re-
93 colonised by the sensitive strain becomes *SR* or *S* with equal probability (**Fig.**
94 **2b**). Because dual carriers maintain carriage of both sensitive and resistant
95 strains in equal measure, we refer to this model as the "within-host balancing"
96 model. Lipsitch and colleagues[10] showed that balancing and knockout are
97 required for this dual carriage model to be "structurally neutral". That is, if strain
98 one and strain two are identical in all but label, when a small number of strain-
99 two carriers is introduced into a population primarily consisting of strain-one
100 carriers, a structurally neutral model would not predict that strain-two carriers
101 increase in frequency to reach some stable equilibrium prevalence (*e.g.*, 50%);
102 since the strains are equivalent, this behaviour would indicate that coexistence
103 follows from unspecified assumptions of the model structure. The within-host
104 balancing model produces coexistence, which increases with the relative
105 efficiency of co-colonisation, k (**Fig. 2c**), consistent with the role of negative
106 frequency dependence outlined above. However, it does not permit enough
107 coexistence to capture observed resistance patterns in bacteria such as
108 *Streptococcus pneumoniae* (**Fig. 2d**), even when co-colonisation is more efficient
109 than single colonisation ($k > 1$; **Supplementary Information**).
110
111 Although the within-host balancing model is structurally neutral at the between-
112 host level, we argue that its balancing and knockout mechanisms contradict the

113 principle of structural neutrality at the within-host level. That is, if a small
114 amount of an invading strain colonises a host already carrying a larger,
115 established resident population, the within-host balancing model assumes that
116 the invading strain increases in frequency to reach an equal proportion to that of
117 the resident strain. Moreover, if a dual carrier is re-colonised, this process
118 repeats, with the host losing one of its two existing strains. To overcome these
119 violations of structural neutrality at the within-host level, we developed a
120 "within-host neutral" model by including two dual carrier states: S_R and R_S, who
121 primarily carry the sensitive or resistant strain with a small complement of
122 resistant or sensitive bacteria, respectively (**Fig. 2e**). In this new model, a strain
123 invading an already-colonised host does not immediately reach an equal
124 proportion with the resident strain, it does not knock out any resident strains,
125 and it is not transmitted further due to its relatively small frequency (**Fig. 2f**).
126 While knockout is required in the within-host balancing model to maintain
127 symmetry of colonisation events, it also has the effect of reducing the frequency
128 of dual carriage, because knockout reduces strain diversity within hosts.
129 Accordingly, incorporating within-host neutrality substantially increases
130 coexistence between sensitive and resistant strains (**Fig. 2g**) without violating
131 structural neutrality at the population level. Moreover, by calibrating the within-
132 host neutral model to empirical data, we show that it readily captures *S.*
133 *pneumoniae* resistance prevalence across 27 European countries (**Fig. 2h**). In
134 reality, there is an indefinite number of dual carriage frequencies corresponding
135 to different ratios of susceptible and resistant strain densities within the host.
136 However, our simple two-state dual carriage model reproduces the simulation

137 results of a more complex individual-based model that allows for arbitrary
138 within-host strain frequencies (**Fig. 2g**).
139
140 Both the standard within-host balancing and our within-host neutral models
141 distinguish sensitive from resistant strains by assuming the latter has a reduced
142 transmission rate. By assuming instead that the two strains differ in their within-
143 host fitness[17, 18], such that a resistant strain will, in the absence of antibiotic
144 treatment, be outcompeted by a sensitive stain, we add within-host succession to
145 the neutral model. We capture within-host succession by allowing R_S hosts to
146 become S_R hosts at rate b (i.e., the higher growth rate of the sensitive strain
147 allows it to outcompete the resistant strain within the host), and remove the
148 transmission cost, c, for resistant strains (**Fig. 2i, j**). Including within-host
149 competition expands the parameter space over which coexistence is maintained
150 (**Fig. 2k**), with the largest range of coexistence found when immunity to
151 reinfection is low (k = 1). Succession further promotes coexistence by
152 strengthening frequency dependence, adding a new mechanism under which
153 sensitive strains also have a fitness advantage when rare, because sensitive cells
154 colonising an R carrier can grow over time to become the dominant strain in the
155 host. Again, this relative advantage dissipates as S carriers become more
156 common, since sensitive cells have a lower probability of colonising an R carrier;
157 together, this yields frequency-dependent fitness advantages for both the
158 sensitive and resistant strains. The neutral model with succession yields an
159 improved model fit to the same *S. pneumoniae* resistance data (**Fig. 2l**). This
160 result is robust to feasible assumptions concerning the loss of resistant cells
161 from S_R hosts (**Supplementary Information**).

162

163 Finally, to evaluate the robustness of our results across other bacteria-antibiotic
164 combinations, we re-parameterised all three models for two additional
165 facultatively pathogenic bacterial species, *Escherichia coli* and *Staphylococcus*
166 *aureus* (**Supplementary Information**). We then recalibrated the suite of models
167 to pan-European data on resistance prevalence against the most widely used
168 antibiotics for all three species (**Fig. 3**). Consistent with the results for *S.*
169 *pneumoniae* penicillin non-susceptibility (**Fig. 2 d,h,l**), the trends observed over
170 the further four bacteria-antibiotic combinations are better captured by both the
171 within-host neutral models than by the within-host balancing model (**Fig. 3**).
172 When selecting the model that gives the statistical best fit to these data, the
173 neutral model with succession has the most support under all bacteria-drug
174 combinations (**Figs. 2, 3**).
175

176 Existing mathematical models have not convincingly replicated empirical trends
177 of resistance prevalence. Although a number of mechanisms that could explain
178 coexistence between drug-sensitive and resistant pathogens have been
179 proposed[6–9, 20, 21], some only support modest amounts of coexistence[7, 9], while the
180 mechanisms proposed have been potentially difficult to generalize empirically,
181 such as specific immune responses to resistance determinants[7], strongly age-
182 assortative mixing[7], or independent mappings of balancing selection[8]. Here we
183 find that incorporating structural neutrality at the within-host scale resolves this
184 incompatibility for the first time by providing a single generalizable mechanism
185 for co-existence across a range of important bacteria-drug combinations.
186

187 Our class of structurally neutral models provides two advances on previous
188 work. First, it captures structural neutrality at the within-host level, thereby
189 harmonising the epidemiology and the within-host dynamics. Second, unlike
190 previous models, this new class better captures observed patterns of resistance
191 prevalence and does so parsimoniously. Our proposed models rely on dual
192 carriage of resistant and sensitive strains, which is generated in our models
193 through co-colonisation. An alternative mechanism through which dual carriage
194 could occur is frequent mutation, which would itself promote coexistence
195 through both mutation-selection balance and an increase in the prevalence of
196 dual carriage. The extent to which dual carriage may drive coexistence of
197 resistant and sensitive strains is an empirical proposition, and will best be
198 answered through a combination of modelling and empirical observation. The
199 empirical prevalence of dual carriage is not well known, but a study of *S. aureus*
200 carriage in children found 21% of hosts carried both resistant and sensitive
201 strains[22] and—although resistance phenotypes were not measured—other
202 studies have found up to 48% multiple carriage of genetically-distinct *S.*
203 *pneumoniae* strains[23, 24] and 42% multiple carriage of virulent *E. coli* strains[25].
204 These studies find that carriage is typically dominated by one strain with other
205 strains carried at low frequency, consistent with our model structure. While it is
206 possible that coexistence is maintained by forces additional to dual carriage, we
207 suggest that any model that incorporates dual carriage should also integrate
208 within-host neutrality to avoid biasing the model against coexistence.
209
210 Although our mathematical models are robust across multiple bacteria-antibiotic
211 combinations[3–5], there are bacteria-specific mechanisms that should be noted.

212 For example, to more accurately quantify *S. pneumoniae* carriage and the spread
213 of resistance, particularly in the era of pneumococcal conjugate vaccines (PCVs),
214 mathematical models would ideally integrate serotype dynamics[9, 26, 27].
215 Moreover, it is clear that there is substantial between-country variation in
216 resistance prevalence that the models analysed here do not capture. Part of this
217 variation is likely to stem from differences in the frequency of person-to-person
218 transmission as well as disease- and age-specific antibiotic treatment rates[9].
219 Other variation across countries may occur from importation of resistant or
220 sensitive strains from sources including travel outside the country of origin and
221 agricultural transmission. Providing a framework in which to answer public
222 health questions will require a balance between mathematical tractability and
223 identifiability of the models on one side, and necessary complexity on the other.
224 Building on the simple models proposed here will help to establish that balance.
225
226 Without a clear mechanistic understanding of the spread of antimicrobial
227 resistance, it will be difficult to disentangle the complex suite of factors that are
228 likely to affect the global prevalence of resistance. If mathematical models are
229 able to incorporate a truly mechanistic understanding of resistance, they will be
230 better able to explain common patterns of resistance and to accurately predict
231 the effect of interventions at a national and global level[28]. With growing calls for
232 an integrated and multifaceted approach to the problem of antimicrobial
233 resistance[1, 2], a new generation of mechanistic mathematical models will be
234 uniquely placed to support the evidence-based adoption of impactful and cost-
235 effective strategies.

Methods

Single-carriage model — The single-carriage model is given by

$$\frac{dS}{dt} = \beta SX - (u + \tau)S$$

$$\frac{dR}{dt} = \beta(1 - c)RX - uR$$

$$X = 1 - S - R\,. \qquad (1)$$

Here, $S = S(t)$ is the fraction of sensitive strain carriers in the population; $R = R(t)$ is the fraction of resistant strain carriers in the population; and $X = X(t)$ is the fraction of non-carriers. The parameter β is the person-to-person transmission rate of the sensitive strain, u is the natural clearance rate, τ is the per capita rate of antibiotic treatment, and c is the transmission cost of resistance.

Within-host balancing model — Following previous work[7, 10], the balancing model is given by

$$\frac{dS}{dt} = \beta S_{tot}X - (u + \tau)S - k\beta(1 - c)R_{tot}S + \frac{k\beta S_{tot}D}{2}$$

$$\frac{dR}{dt} = \beta(1 - c)RX - uR - k\beta S_{tot}R + \frac{k\beta(1-c)R_{tot}D}{2} + \tau D$$

$$\frac{dD}{dt} = k\beta(1 - c)R_{tot}S + k\beta S_{tot}R - (u + \tau)D - k\beta S_{tot}D - k\beta(1 - c)R_{tot}D$$

$$X = 1 - S - R - D\,. \qquad (2)$$

Here, the additional compartment $D = D(t)$ is the fraction of dual carriers in the population (*SR* carriers in the main text), k is the efficiency of multiple

colonisation relative to single colonisation, and $S_{tot} = S + D/2$ and $R_{tot} = R + D/2$ give the effective population burden of sensitive- and resistant-strain colonisation, respectively. The resistance prevalence is given by $\rho = R_{tot}/(1-X)$.

Within-host neutrality model — The novel neutral model is given by

$$\frac{dS}{dt} = \beta(S + S_R)X - (u + \tau)S - k\beta RS$$

$$\frac{dS}{dt} = \beta(1 - c)RX - uR + \tau S_R$$

$$\frac{dR}{dt} = \beta(1 - c)RX - uR + \tau S_R$$

$$\frac{dS_R}{dt} = k\beta(1 - c)RS - (u + \tau)S_R$$

$$X = 1 - S - R - S_R\,. \qquad (3)$$

Here, the compartment $S_R = S_R(t)$ captures the fraction of the population predominantly colonised with sensitive bacteria, but also carrying a small amount of resistant bacteria, and $S + S_R$ gives the effective population burden of sensitive-strain colonisation. The $R_S = R_s(t)$ compartment shown in **Fig. 2e** is omitted as it does not impact upon the overall resistance prevalence in this model, $\rho = R/(1-X)$.

Within-host neutrality model with succession — Finally, the neutral model with succession is given by

$$\frac{dS}{dt} = \beta(S + S_R)X - (u + \tau)S - k\beta(R + R_S)S$$

283 $$\frac{dR}{dt} = \beta RX - uR + \tau(S_R + R_S) - k\beta(S + S_R)R$$

284 $$\frac{dS_R}{dt} = k\beta(R + R_S)S - (u + \tau)S_R + bR_S$$

285 $$\frac{dR_S}{dt} = k\beta(S + S_R)R - (u + \tau)R_S - bR_S$$

286 $$X = 1 - S - R - S_R - R_S\,. \qquad (4)$$

287

288 Here, the R_S compartment captures dual carriers predominantly colonised with
289 resistant bacteria plus a small amount of sensitive bacteria, and b captures the
290 within-host benefit of sensitivity.

291

292 *Ordinary differential equation solutions* — All models are solved by setting single-
293 carriage compartments (S and R) equal to 0.001 and all dual-carriage
294 compartments to 0, then integrating the systems of ordinary differential
295 equations numerically using the Runge–Kutta Dorman–Prince method until they
296 reach equilibrium. All models were simulated using C++.

297

298 *Model parameterisation and calibration* — We calibrated the models using
299 European Centre for Disease Prevention and Control data on penicillin
300 consumption[3] and the prevalence of penicillin non-susceptibility among *S.*
301 *pneumoniae* invasive isolates[4] from 2007 for 27 European countries. We focused
302 on the year 2007 for this data set as criteria for penicillin non-susceptibility in *S.*
303 *pneumoniae* were changed in some countries after this year, yielding
304 inconsistencies in resistance data between countries[7, 28]. For calibration to all
305 other bacteria-drug combinations, we used data for the same 27 countries
306 collected in 2015, the most recent year for which data are available[3, 5]. Antibiotic

consumption rates were given in defined daily doses (DDD) per thousand people; we converted these to overall treatment rates by assuming that 10 DDD comprise one treatment course for penicillin[8] and fluoroquinolones, while 7 DDD comprise one treatment course for macrolides.

We used Markov chain Monte Carlo with differential evolution[30] to calibrate the model output to empirical data. We assumed that the number of resistant isolates tested in a given country follows a binomial distribution with success probability drawn from a beta distribution, with the model-predicted resistance prevalence as the mode of the beta distribution. Setting the success probability as a random variable allowed us to account for between-country variation in resistance prevalence not captured by our dynamic model. The likelihood of the observed resistance prevalence for bacteria-antibiotic set j across all countries, $\boldsymbol{d_j}$, given the model predicted resistance prevalence, ρ_j, and prevalence of carriage, Y_j, is

$$L_j\left(\boldsymbol{d_j}\middle|\rho_j, \boldsymbol{Y_j}\right) = \prod_{i=1}^{c_j}\left(\left[Y_j^{(0)} \leq Y\left(\tau_{i,j}\right) \leq Y_j^{(1)}\right]\int_{x=0}^{1}\mathrm{Beta}\left(x\middle|\omega = \rho_j\left(\tau_{i,j}\right), \kappa = \kappa_j^*\right)\mathrm{Bin}\left(r_{i,j}\middle|n_{i,j}, x\right)dx\right).$$

Here, $\left[Y_j^{(0)} \leq Y\left(\tau_{i,j}\right) \leq Y_j^{(1)}\right]$ is 1 if $Y(\tau_{i,j})$ lies between $Y_j^{(0)}$ and $Y_j^{(1)}$, which are the lower and upper bounds of duration of carriage, respectively, and 0 otherwise; $\mathrm{Beta}(x|\omega,\kappa) = x^{\alpha-1}(1-x)^{\beta-1}\Gamma(\alpha+\beta)/(\Gamma(\alpha)\Gamma(\beta))|_{\alpha = \omega(\kappa-2) + 1,\ \beta = (1-\omega)(\kappa-2)+1}$ is the beta distribution probability density with mode ω and concentration κ; and

$\mathrm{Bin}(r|n,x) = \binom{n}{r} x^r (1-x)^{n-r}$ is the binomial distribution probability density. There are C_j countries in the data set j labelled $i = 1 \ldots C_j$; for a country i and bacteria-antibiotic set j, the measured antibiotic use is $\tau_{i,j}$, the number of samples taken of a particular bacteria is $n_{i,j}$, and the number of those samples tested as non-susceptible to the particular antibiotic is $r_{i,j}$. The model prediction for resistance prevalence given treatment rate τ is $\rho_j(\tau)$, the model prediction for prevalence of carriage given treatment rate τ is $Y_j(\tau)$, and the estimated concentration around the best-fit line, estimated from the data, is κ_j^*.

To estimate the concentration κ_j^* from the resistance prevalence data, we used a truncated line function $f(\tau) = \max(0, a + g\tau)$ as the modal antibiotic resistance prevalence and fixed κ_j^* as the concentration. We calculated the maximum likelihood estimates of a_j^*, g_j^*, and κ_j^* by using the Nelder-Mead algorithm[31] to maximize the following likelihood function:

$$L_j^{(1)}(a_j^*, g_j^*, \kappa_j^*) = \prod_{i=1}^{C_j} \int_{x=0}^{1} \mathrm{Beta}\left(x \middle| \omega = \max\left(0, a_j^* \tau_{i,j} + g_j^*\right), \kappa = \kappa_j^*\right) \mathrm{Bin}\left(r_{i,j} \middle| n_{i,j}, x\right) dx$$

Priors for all model fitting were identified from the literature and were bacteria-specific (**Supplementary Information**).

For illustrative purposes, the parameters c and b for **Fig. 2c, g, k** were chosen such that τ = 1.5 courses per person per year would lead to 50% resistance

349 prevalence (**Fig. 3a-c)**. This τ was chosen to roughly coincide with *S. pneumoniae*

350 empirical data[3, 5]. Other parameters used were $\beta = 4$, $u = 1$ (ref. 7) and k as given

351 in the figure.

352

353 *Individual-based model* — In the individual-based model, hosts are indexed by

354 $i \in 1 \ldots N$, where N is the population size. Each host is characterised by a pair of

355 real numbers (s_i, r_i) giving the normalised load of sensitive and resistant bacteria

356 colonising the host ($s_i = r_i = 0$ in uncolonised hosts, while $s_i + r_i = 1$ in colonised

357 hosts). A new sensitive-strain colonisation changes a host's bacterial load to (s_i',

358 r_i') = $((s_i + \iota)/(s_i + r_i + \iota), r_i/(s_i + r_i + \iota))$, while a new resistant-strain colonisation

359 changes a host's bacterial load to $(s', r') = (s/(s + r + \iota), (r + \iota)/(s + r + \iota))$, where ι

360 << 1 is the germ size. The rate at which hosts experience new colonisations is λ_S

361 $= \beta \Sigma_i s_i$ for sensitive colonisations and $\lambda_R = \beta(1-c) \Sigma_i r_i$ for resistant colonisations.

362 Hosts receive treatment at rate τ, which sets their (s_i', r_i') = (0, r_i), and experience

363 natural clearance at rate u, which sets their (s_i', r_i') = (0, 0). The model proceeds

364 in discrete time steps of 0.001 months.

365 **References**

366

367 1. World Health Organization. *United Nations high-level meeting on antimicrobial*
368 *resistance.*
369 http://www.who.int/antimicrobial-resistance/events/UNGA-meeting-amr-
370 sept2016/en (2016).
371 2. O'Neill J, *ed*. *Tackling drug-resistant infections globally: final report and*
372 *recommendations*. https://amr-review.org/home.html (2016).
373 3. European Centre for Disease Prevention and Control. Antimicrobial
374 consumption rates by country.
375 http://ecdc.europa.eu/en/healthtopics/antimicrobial-resistance-and-
376 consumption/antimicrobial-consumption/esac-net-
377 database/Pages/Antimicrobial-consumption-rates-by-country.aspx (2017).
378 4. European Antimicrobial Resistance Surveillance System. *EARSS Annual Report*
379 *2007*. Bilthoven: EARSS.
380 5. European Centre for Disease Prevention and Control. *Antimicrobial resistance*
381 *surveillance in Europe 2015. Annual Report of the European Antimicrobial*
382 *Resistance Surveillance Network (EARS-Net)*. Stockholm: ECDC (2017).
383 6. Austin DJ, Kristinsson KG, Anderson RM. The relationship between the volume
384 of antimicrobial consumption in human communities and the frequency of
385 resistance. *Proc Natl Acad Sci USA* **96**, 1152–1156 (1999).
386 7. Colijn C, *et al.* What is the mechanism for persistent coexistence of drug-
387 susceptible and drug-resistant strains of *Streptococcus pneumoniae*? *J. R. Soc.*
388 *Interface* **7**, 905–919 (2010).

389 8. Lehtinen S, *et al.* Evolution of antibiotic resistance is linked to any genetic
390 mechanism affecting bacterial duration of carriage. *Proc Natl Acad Sci USA* **114**,
391 1075–1080 (2017).
392 9. Cobey S, *et al.* Host population structure and treatment frequency maintain
393 balancing selection on drug resistance. *J R Soc Interface* **14**, 20170295 (2017).
394 10. Lipsitch M, Colijn C, Cohen T, Hanage WP, Fraser C. No coexistence for free:
395 neutral null models for multistrain pathogens. *Epidemics* **1**, 2–13 (2009).
396 11. Hardin G. The competitive exclusion principle. *Science* **131**, 1292–1297
397 (1960).
398 12. Ayala FJ, Campbell CA. Frequency-dependent selection. *Ann Rev Ecol Syst* **5**,
399 115–138 (1974).
400 13. Ayala FJ. Competition between species: frequency dependence. *Science* **171**,
401 820–824 (1971).
402 14. Sinervo B, Lively CM. The rock-paper-scissors game and the evolution of
403 alternative male strategies. *Nature* **380**, 240–243 (1996).
404 15. Gigord LDB, Macnair MR, Smithson A. Negative frequency-dependent
405 selection maintains a dramatic flower color polymorphism in the rewardless
406 orchid *Dactylorhiza sambucina* (L.) Soò. *Proc Natl Acad Sci USA* **98**, 6253–6255
407 (2001).
408 16. Rainey PB, Travisano M. Adaptive radiation in a heterogeneous environment.
409 *Nature* **394**, 69–72 (1998).
410 17. Andersson DI. The biological cost of mutational antibiotic resistance: any
411 practical conclusions? *Curr Opin Microbiol* **9**, 461–465 (2006).
412 18. Andersson DI, Hughes D. Antibiotic resistance and its cost: is it possible to
413 reverse resistance? *Nat Rev Microbiol* **8**, 260–271 (2010).

414 19. Lipsitch M. Vaccination against colonizing bacteria with multiple serotypes.
415 *Proc Natl Acad Sci USA* **94**, 6571–6576 (1997).
416 20. Dietz K. Epidemiologic interference of virus populations. *J Math Biol* **8**, 291–
417 300 (1979).
418 21. Gupta S, Swinton J, Anderson RM. Theoretical studies of the effects of
419 heterogeneity in the parasite population on the transmission dynamics of
420 malaria. *Proc R Soc Lond B* **256**, 231–238 (1994).
421 22. Mongkolrattanothai K, *et al.* Simultaneous carriage of multiple genotypes of
422 *Staphylococcus aureus* in children. *J Med Microbiol* **60**, 317–322 (2011).
423 23. Kamng'ona AW, *et al.* High multiple carriage and emergence of *Streptococcus*
424 *pneumoniae* vaccine serotype variants in Malawian children. *BMC Inf Diseases* **15**,
425 234 (2015).
426 24. Turner P, *et al.* Improved detection of nasopharyngeal cocolonization by
427 multiple pneumococcal serotypes by use of latex agglutination or molecular
428 serotyping by microarray. *J Clin Microbiol* **49**, 1784–1789 (2011).
429 25. Martinez-Medina M, *et al.* Molecular diversity of *Escherichia coli* in the human
430 gut: new ecological evidence supporting the role of adherent-invasive *E. coli*
431 (AIEC) in Crohn's disease. *Inflamm Bowel Dis* **15**, 872–882 (2009).
432 26. Cobey S, Lipsitch M. Niche and neutral effects of acquired immunity permit
433 coexistence of pneumococcal serotypes. *Science* **335**, 1376–1380 (2012).
434 27. Flasche S, *et al.* The impact of specific and non-specific immunity on the
435 ecology of *Streptococcus pneumoniae* and the implications for vaccination. *Proc R*
436 *Soc B* **280**, 20131939 (2013).
437 28. Atkins KE, *et al.* Use of mathematical modelling to assess the impact of
438 vaccines on antibiotic resistance. *Lancet Infect Dis* (in press).

439

440 *Additional references for Methods*

441

442 29. Goossens MC, Catry B, Verhaegen J. Antimicrobial resistance to
443 benzylpenicillin in invasive pneumococcal disease in Belgium, 2003–2010: the
444 effect of altering clinical breakpoints. *Epidemiol Infect* **141**, 490–495 (2013).
445 30. Ter Braak CJF. A Markov chain Monte Carlo version of the genetic algorithm
446 differential evolution: easy Bayesian computing for real parameter spaces. *Stat*
447 *Comp* **16**, 239-249 (2006).
448 31. Nelder JA, Mead R. A simplex method for function minimization. *Comp J* **7**,
449 308–313 (1965).

450

Supplementary Information is included at the end of this document.

Acknowledgments. We thank M. Davies for assistance. NGD, MJ and KEA were funded by the National Institute for Health Research Health Protection Research Unit (NIHR HPRU) in Immunisation at the London School of Hygiene and Tropical Medicine in partnership with Public Health England (PHE). The views expressed are those of the authors and not necessarily those of the NHS, the NIHR, the Department of Health or Public Health England.

Author contributions. NGD, SF, MJ and KEA conceived the study. NGD performed the analyses. NGD and KEA drafted the manuscript, which all authors revised.

The authors declare no competing financial interests.

Correspondence and requests for materials should be addressed to Nicholas.Davies@lshtm.ac.uk.

468 **Figures**

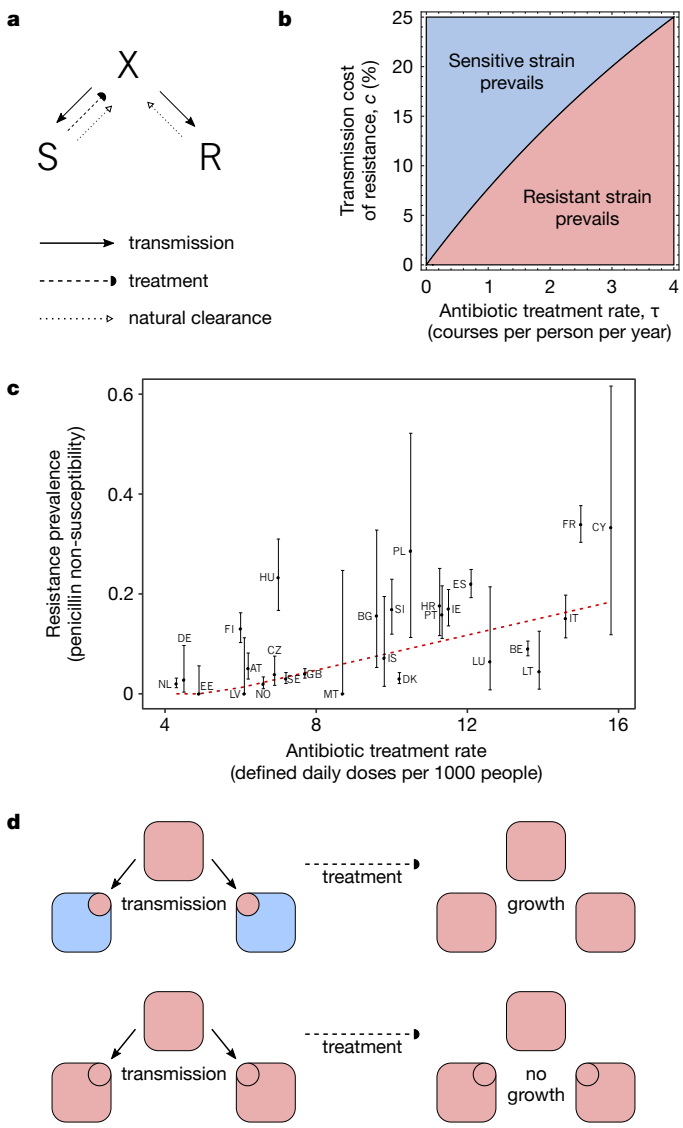

469

470 **Figure 1 | The problem of coexistence. (a)** Observed prevalence of penicillin

471 non-susceptibility in invasive isolates of *S. pneumoniae* across 27 European

472 countries, illustrating widespread coexistence. **(b)** A simple two-strain single

473 carriage model defined by the system of ordinary differential equations

474 $\frac{dD}{dt} = \beta SX - (u + \tau)S, \frac{dR}{dt} = \beta(1 - c)RX - uR, X = 1 - S - R$. Here, β is the rate of

475 transmission (solid arrows), u is the rate of natural clearance (dotted arrows), τ

476 is the rate of antibiotic treatment (dashed arrow), and c is the cost of resistance.

(c) The single carriage model produces competitive exclusion, with the sensitive strain dominating the resistant strain if $c > \tau/(u + \tau)$. The region plot shows outcomes when $\beta = 4$ months^{-1}, $u = 1$ months^{-1}. **(d)** Dual carriage allows coexistence by promoting frequency-dependent selection on the resistant strain. When the sensitive strain is relatively common, resistant-strain carriers (red boxes) are more likely to transmit bacteria to sensitive-strain carriers (blue boxes). If the resulting co-colonised carriers are then treated with antibiotics, the resistant strain grows within the host to take the place of the killed sensitive cells. Overall, this gives the resistant strain a fitness advantage when it is rare. As the resistant strain becomes more common, it is less likely to colonise a sensitive-strain carrier, diminishing the resistant strain's frequency-dependent fitness advantage.

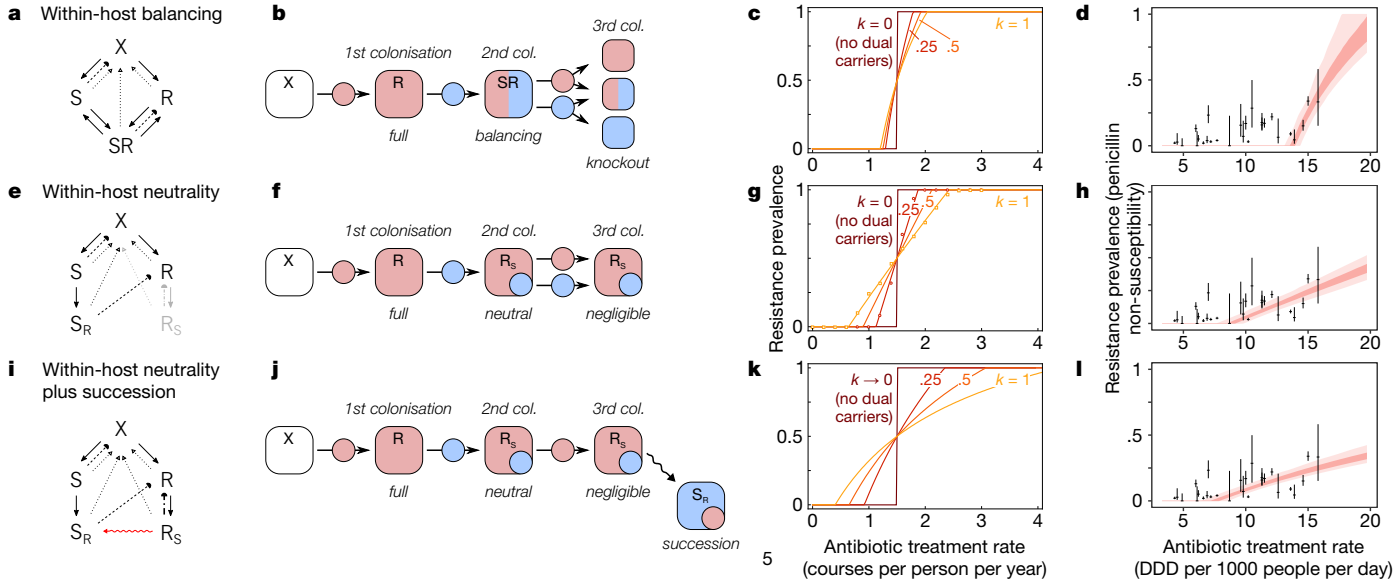

Figure 2 | Models of dual carriage. (a)–(d) The within-host balancing model[10]. **(a)** The two-strain model (**Fig. 1b**) is extended by the addition of a dual-carrier compartment, SR. The parameter k gives the relative efficiency of transmission to an already-colonised host; $k = 0$ eliminates dual carriage and recovers the two-strain model. **(b)** An example sequence of colonisation events under the within-host balancing model, illustrating equal co-colonisation and knockout. **(c)** Although coexistence increases with the efficiency of multiple carriage, k, the region of coexistence remains small for the within-host balancing model. **(d)** The within-host balancing model provides a poor fit to penicillin non-susceptibility in *S. pneumoniae* across European countries. **(e)** The within-host neutral model features two dual-carriage components, S_R and R_S, reflecting the relative dominance of a given strain within hosts. This model is structurally neutral at both the population and the within-host level. **(f)** The same example sequence of colonisation events as in panel **b** illustrates the absence of the balancing and knockout mechanisms. **(g)** Integrating within-host neutrality expands the region of coexistence. Overlaid markers are results from an individual-based model

with an arbitrary number of co-colonisation states (see **Methods**) for k = 0.25 and k = 1, showing agreement with the two-state co-colonisation model shown in panel **e**. **(h)** Within-host neutrality provides a better fit to empirical data. **(i)** The within-host neutral model with succession allows the sensitive strain to outcompete the resistant strain within the host at rate b. **(j)** The same example sequence illustrates frequency-dependent selection acting on the sensitive strain. **(k)** Including within-host competition further increases coexistence and **(l)** the resulting model provides the best fit to the data. Relative likelihoods were calculated as 4.49×10^{-5} for the within-host balancing model and 0.635 for the neutral model (relative to the neutral model with succession).

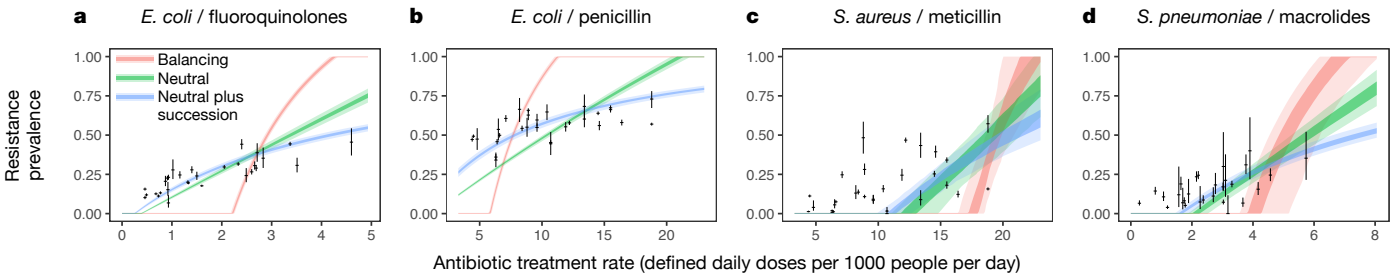

Figure 3 | Model fit to additional bacteria-drug combinations. Within-host neutral models with (blue) or without (green) succession outperform the balancing model (red). **(a)** *E. coli*, fluoroquinolone resistance. The balancing model has likelihood 2.45×10^{-127}, and the neutral model 3.85×10^{-15}, relative to the neutral model with succession. **(b)** *E. coli*, penicillin resistance. Relative likelihoods are 3.22×10^{-163} for the balancing model and 3.41×10^{-28} for the neutral model. **(c)** *S. aureus*, meticillin resistance. Relative likelihoods are 6.33×10^{-4} for the balancing model and 0.141 for the neutral model. **(d)** *S. pneumoniae*, macrolide resistance. Relative likelihoods are 6.57×10^{-15} for the balancing model and 2.28×10^{-3} for the neutral model.

Supplementary information for:

Within-host dynamics explain the coexistence of antibiotic-sensitive and resistant bacteria

Nicholas G. Davies[1,2], *Stefan Flasche*[1,2], *Mark Jit*[1,2,3], *Katherine E. Atkins*[1,2]

[1]Centre for Mathematical Modelling of Infectious Diseases, London School of Hygiene and Tropical Medicine, London, UK

[2]Department for Infectious Disease Epidemiology, Faculty of Epidemiology and Population Health, London School of Hygiene and Tropical Medicine, London, UK

[3]Modelling and Economics Unit, Public Health England, London, UK

Corresponding Author: Nicholas.Davies@lshtm.ac.uk

Table of Contents

1. Sources for antibiotic consumption and resistance prevalence data **2**

2. Details of model fitting **3**

Priors for duration of carriage *3*

Likelihood ranges for carriage prevalence *4*

MCMC details *5*

3. Posterior distributions from model fitting **5**

4. Positive association between carriers: $k > 1$ **8**

Posterior distributions from model fitting with $0 \leq k \leq 5$ *9*

Relative likelihoods from model fitting with $0 \leq k \leq 5$ *12*

5. S_R-to-S clearance in within-host neutral model with succession **12**

1. Sources for antibiotic consumption and resistance prevalence data

We used data from the European Centre for Disease Prevention and Control (ECDC) and from the European Antimicrobial Resistance Surveillance Network (EARS-Net) to parameterize our models for the consumption of antibiotics and prevalence of antibiotic resistance in EU countries.

The ECDC provides information on antimicrobial consumption in defined daily doses (DDD) per 1000 inhabitants per day for participating countries, with antimicrobials broken down into categories as classified in the World Health Organisation's (WHO) Anatomical Therapeutic Chemical (ATC) Classification System. Consumption is classified into primary care and hospital use, with the majority of use in primary care. We focus on primary care usage only, as hospital usage data is sparse and we are focusing on community-acquired bacterial carriage. The ECDC releases online publications summarizing consumption data (*e.g.* ECDC 2014) and maintains a queryable online database (ECDC 2017b).

EARS-Net, formerly EARSS, provides information on resistance levels as measured in invasive isolates of various bacterial pathogens isolated from blood and cerebrospinal fluid (EARSS 2007; ECDC 2017a). We assume that invasive isolates are a sample of commensally-carried strains (Lehtinen *et al.* 2017). We summarize the data used and sources for the five data sets analysed (**Tab. S1**).

Data set	Consumption: *ATC code, sector, year, and source*	Resistance: *Pathogen, resistance metric, year, and source*
Streptococcus pneumoniae penicillin resistance, 2007 (Figs. 1–2, main text)	J01C (Beta-lactam antibacterials, penicillins), primary care, 2007 (ECDC 2017b, 2014[†])	*S. pneumoniae*, percentage non-susceptible to penicillin, 2007 (EARSS 2007)
Escherichia coli fluoroquinolone resistance, 2015 (Fig. 3a, main text)	J01MA (Fluoroquinolones), primary care, 2015 (ECDC 2017b)	*E. coli*, percentage resistant to fluoroquinolones, 2015 (ECDC 2017a)
E. coli penicillin resistance, 2015 (Fig. 3b, main text)	J01C (Beta-lactam antibacterials, penicillins), primary care, 2015 (ECDC 2017b)	*E. coli*, percentage resistant to aminopenicillins, 2015 (ECDC 2017a)
Staphylococcus aureus meticillin resistance, 2015 (Fig. 3c, main text)	J01C (Beta-lactam antibacterials, penicillins), primary care, 2015 (ECDC 2017b)	*S. aureus*, percentage resistant to meticillin (MRSA), 2015 (ECDC 2017a)
S. pneumoniae macrolide resistance, 2015 (Fig. 3d, main text)	J01FA (Macrolides), primary care, 2015 (ECDC 2017b)	*S. pneumoniae*, percentage non-susceptible to macrolides, 2015 (ECDC 2017a)

Table S1 | Data sources for antibiotic consumption and antimicrobial resistance across five pathogen-drug combinations. [†]Portugal recorded no penicillin consumption for 2007 in the online ECDC database (ECDC 2017b), but the 2011 ECDC report (ECDC 2014) provides the corrected figure of 11.3 DDD per 1000 inhabitants per day for 2007.

2. Details of model fitting

Priors for duration of carriage

For *S. pneumoniae*, we assume an average duration of carriage of 1 month (Colijn *et al*. 2009), giving a clearance rate u = 1 months^{-1}. For *E. coli*, we assume that the average duration of carriage is 59 days (Li *et al*. 2012) to 98 days (Apisarnthanarak *et al*. 2008),

and accordingly set a uniform prior for u over the range 0.3–0.5 months^{-1}. For *S. aureus*, we assume a duration of carriage of 3.3 months (estimated from ambulatory patients clearing MRSA; Shenoy *et al*. 2014) to 5.9 months (Larsson *et al.* 2011), and accordingly set a uniform prior for u over the range 0.17–0.3 months^{-1}.

The transmission parameter, β, is constrained by the likelihood function (see below), so we set a uniform prior on β wide enough to overlap the full range of observed carriage prevalence, Y, given the range of clearance rates u and treatment rates τ (*i.e.* $Y = 1 - (u + \tau)/\beta$ for the sensitive strain alone, and $Y = 1 - u/(\beta(1-c))$ for the resistant strain alone). Specifically, for *S. pneumoniae*, we use the range 1–6; for *E. coli*, we use the range 1–10; and for *S. aureus*, we use the range 0.1–2.

Likelihood ranges for carriage prevalence

In the main text, we detail how the likelihood function used in model fitting constrains model output such that all countries must exhibit a prevalence of carriage Y such that $Y^{(0)} \leq Y \leq Y^{(1)}$. For *S. pneumoniae*, we follow Colijn *et al.* (2010) in assuming $0.2 \leq Y \leq 0.8$ in children. For *E. coli*, we restrict our attention to extraintestinal pathogenic *E. coli* (ExPEC), a subset of *E. coli* that is responsible for most invasive infections, and assume $0.499 \leq Y \leq 0.942$, which is derived from 95% confidence intervals around the observed prevalence of carriage of ExPEC (9 of 12 healthy control subjects) from Martinez-Medina *et al.* (2009). Finally, for *S. aureus*, we adopt $0.2 \leq Y \leq 0.6$ based on Bogaert *et al.* (2004), which is based on the observed range of *S. aureus* colonization in Dutch children, with a slightly wider range to capture more variation between European countries.

MCMC details

Following the differential evolution MCMC algorithm (Ter Braak 2006), we run 10*n* chains, where *n* is the number of free parameters in the model, *i.e.* 30 for *S. pneumoniae* (for which carriage duration is fixed at 1 month) and 40 for *E. coli* and *S. aureus*, for which carriage duration is not fixed. The burn-in period lasts 1,000 iterations, after which 100,000 samples from the posterior are taken across all chains.

3. Posterior distributions from model fitting

Here, we show the posterior distributions from model fitting from the main analysis (**Fig. S1–S5**)

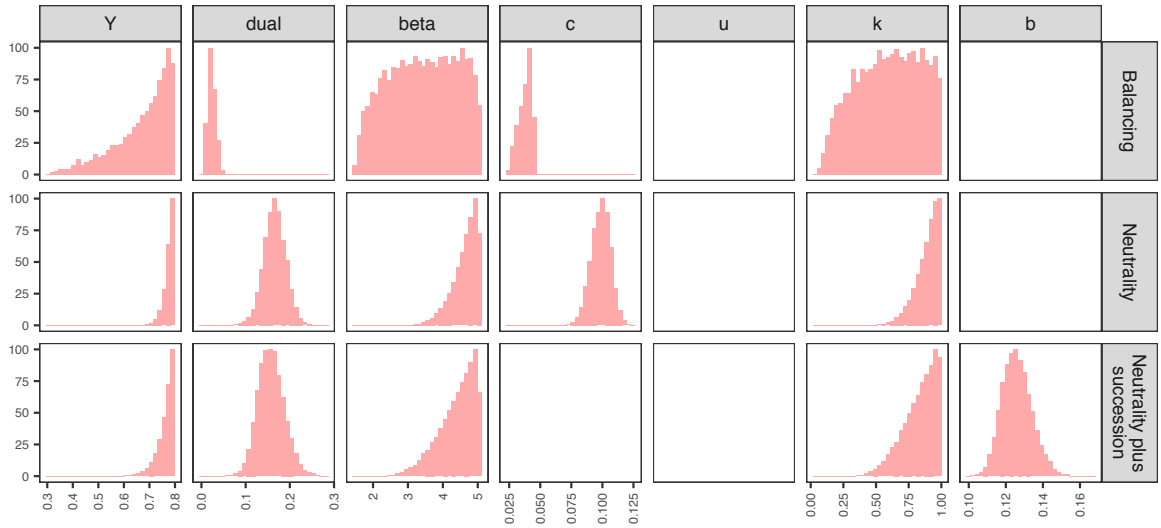

Figure S1 | Posterior distribution for *S. pneumoniae* / penicillin (2007). *Y* gives the overall prevalence of carriage (whether single or dual) in the population; *dual* gives the fraction of carriers who carry both sensitive and resistant strains; *beta* gives the transmission parameter; *c* gives the transmission cost of resistance; *u* gives the clearance rate (if the clearance rate is subject to fitting; for *S. pneumoniae*, *u* = 1); *k* gives the efficiency of recolonisation, and *b* gives the within-host rate of succession (see *Methods*, main text, for details).

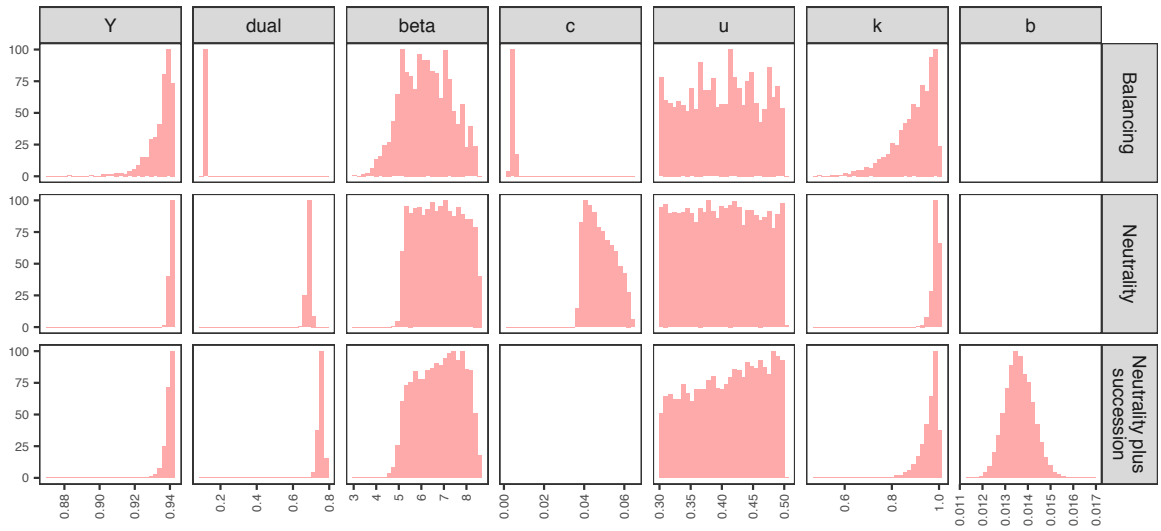

Figure S2 | Posterior distribution for *E. coli* / fluoroquinolones (2015). See Fig. S1 for details.

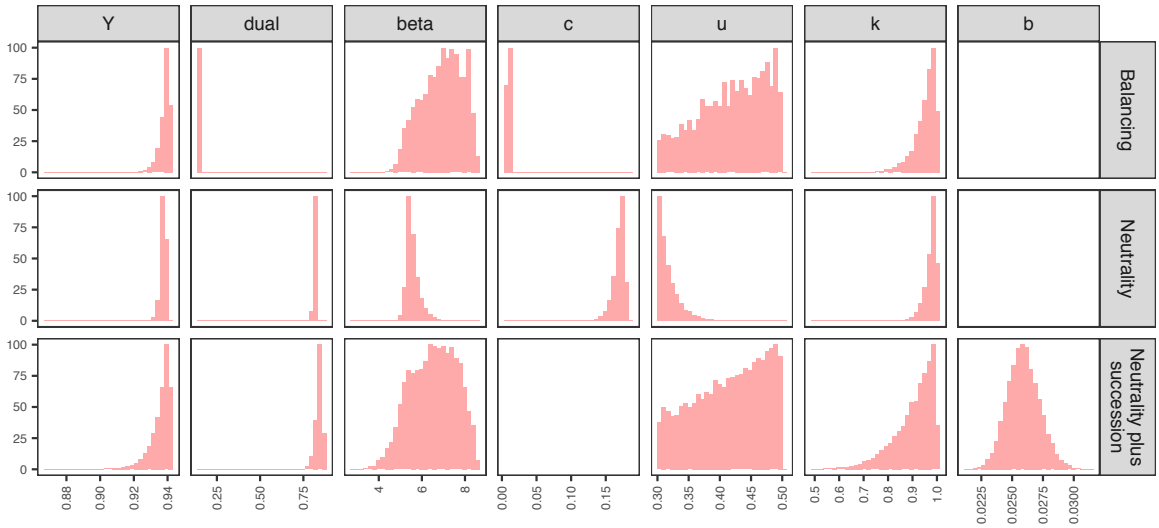

Figure S3 | Posterior distribution for *E. coli* / penicillin (2015). See Fig. S1 for details.

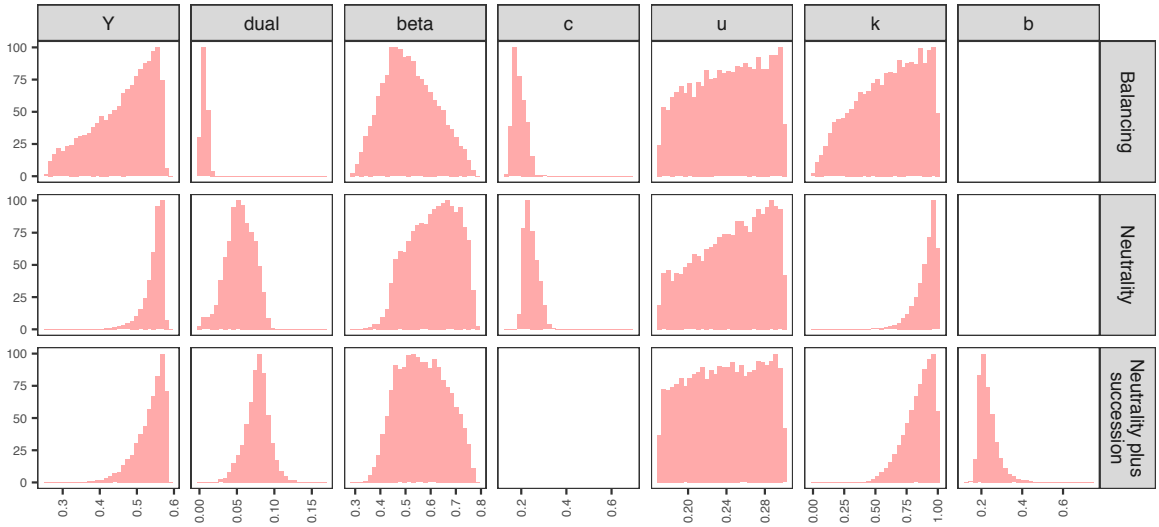

Figure S4 | Posterior distribution for *S. aureus* / meticillin (2015). See Fig. S1 for details.

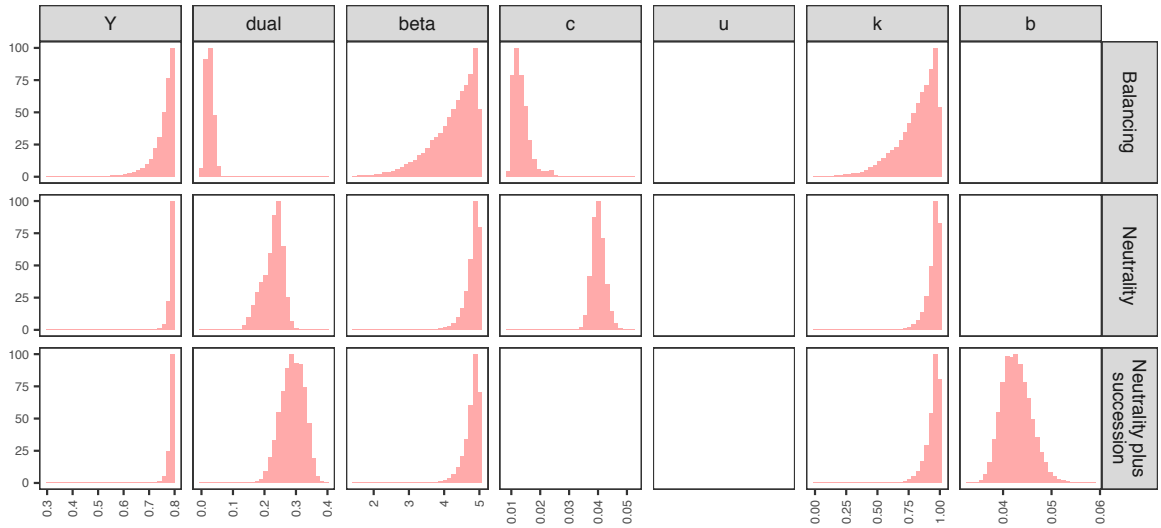

Figure S5 | Posterior distribution for *S. pneumoniae* / macrolides (2015). See Fig. S1 for details.

4. Positive association between carriers: $k > 1$

In the main analysis, we assume that k measures relative efficiency of co-colonisation compared to colonisation of an uncolonised host, and hence restrict our attention to $k \leq 1$. However, it is also possible to interpret k as capturing positive association between carriers, as increasing k increases transmission among carriers without impacting upon the overall prevalence of carriage in the population. Thus, it is possible to have $k > 1$ reflecting this mechanism. Allowing for the range $0 \leq k \leq 5$, we find that (a) the fit of the within-host balancing model does not substantially improve and that (b) similar levels of coexistence are possible for the within-host neutral and within-host succession models with lower prevalence of carriage. Here, for illustration, we adopt more restrictive ranges on the prevalence of carriage: $0.2 \leq Y \leq 0.4$ for *S. pneumoniae*, $0.4 \leq Y \leq 0.8$ for *E. coli*, and $0.2 \leq Y \leq 0.4$ for *S. aureus* (**Fig. S6**).

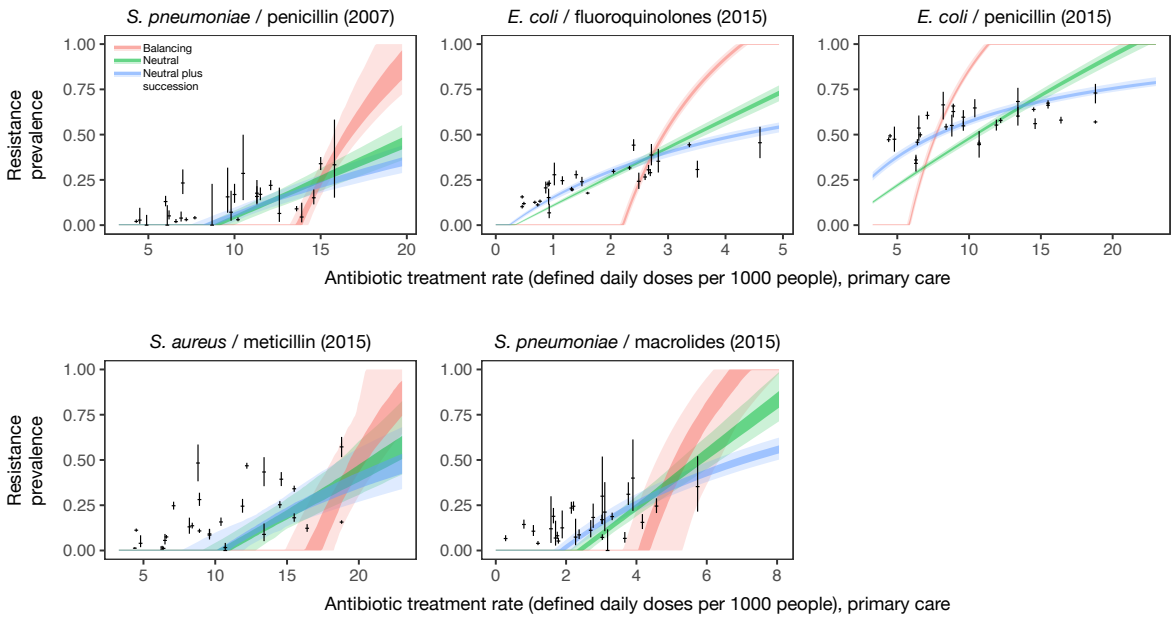

Figure S6 | Model fits with $0 \leq k \leq 5$.

Posterior distributions from model fitting with $0 \leq k \leq 5$

Posterior distributions provided in **Figs. S7–S11**.

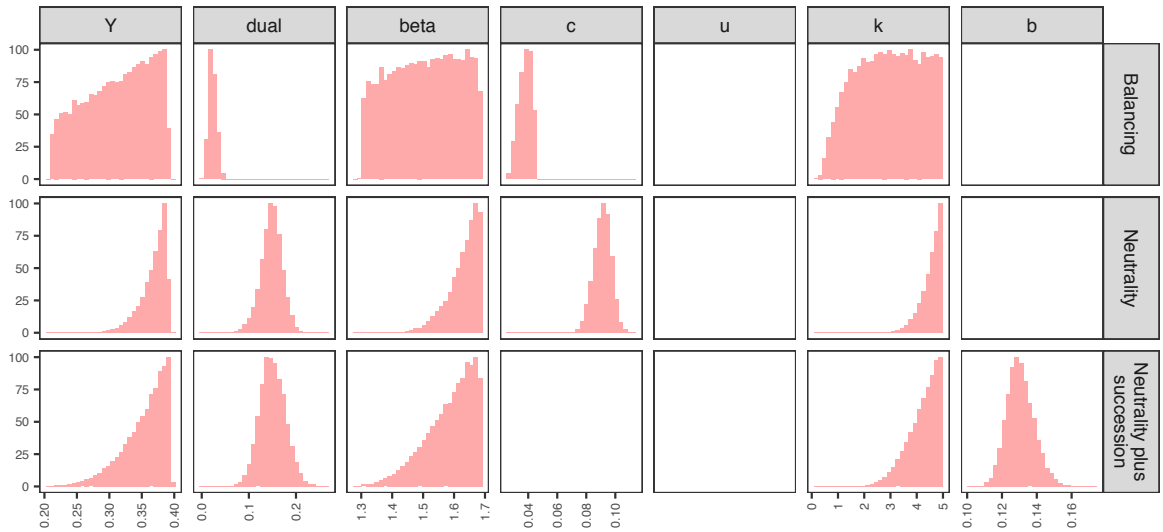

Figure S7 | Posterior distribution for *S. pneumoniae* / penicillin (2007) data set with $0 \leq k \leq 5$.

146

147 **Figure S8 |** Posterior distribution for *E. coli* / fluoroquinolones (2015) data set with $0 \leq$

148 $k \leq 5$.

149

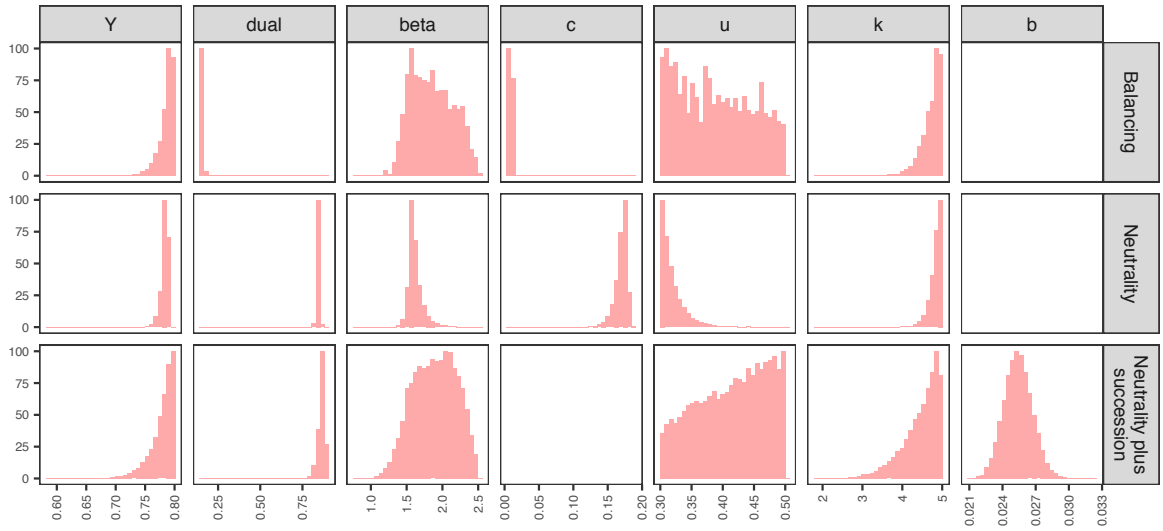

150

151 **Figure S9 |** Posterior distribution for *E. coli* / penicillin (2015) data set with $0 \leq k \leq 5$.

152

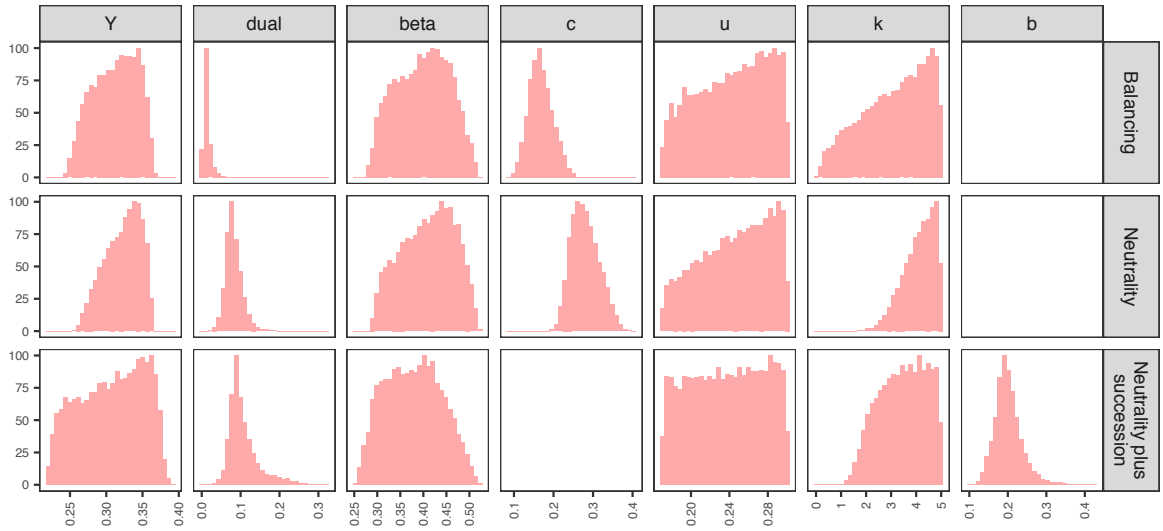

Figure S10 | Posterior distribution for *S. aureus* / meticillin (2015) data set with $0 \leq k \leq 5$.

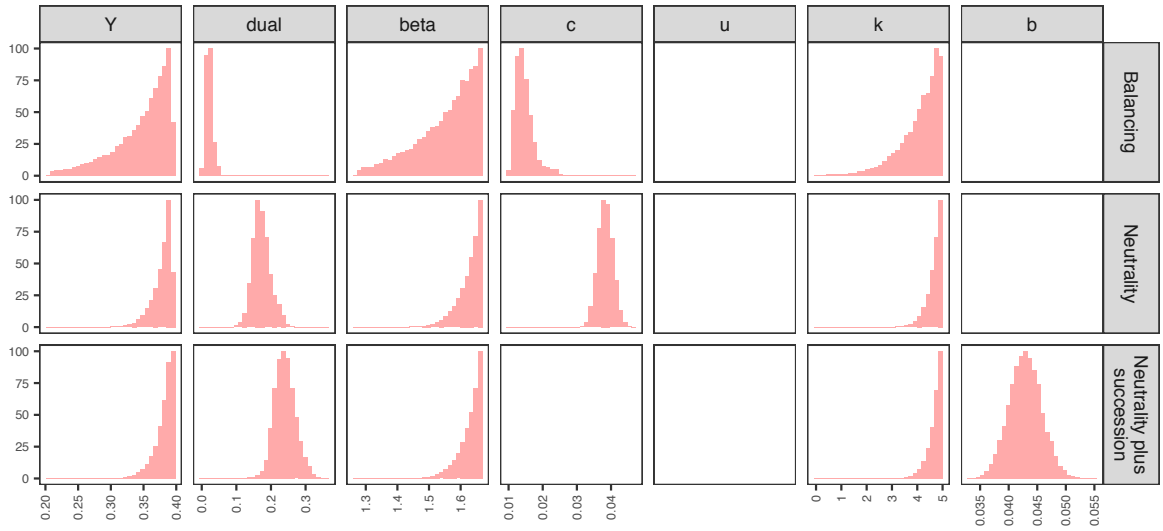

Figure S11 | Posterior distribution for *S. pneumoniae* / macrolides (2015) data set with $0 \leq k \leq 5$.

Relative likelihoods from model fitting with $0 \leq k \leq 5$

We calculated the relative likelihood for the fitted models, M_i, by comparison of the Akaike Information Criterion (AIC) of each model to that of the best model, M ($\exp[(\mathrm{AIC}(M) - \mathrm{AIC}(M_i))/2]$) (**Tab. S2**).

Model	**Within-host balancing**	**Within-host neutrality**	**Within-host neutrality plus succession**
S. pneumoniae / penicillin (2007) (*n* = 3)	4.82×10^{-5}	0.453	1
E. coli / fluoroquinolones (2015) (*n* = 4)	1.11×10^{-127}	1.03×10^{-12}	1
E. coli / penicillin (2015) (*n* = 4)	1.12×10^{-161}	1.34×10^{-26}	1
S. aureus / meticillin (2015) (*n* = 4)	6.87×10^{-4}	0.696	1
S. pneumoniae / macrolides (2015) (*n* = 3)	3.84×10^{-14}	1.33×10^{-3}	1

Table S2 | Relative likelihoods for model fits with $0 \leq k \leq 5$. The number of parameters, *n*, is given for each model.

5. S_R-to-S clearance in within-host neutral model with succession

In the within-host neutral model with succession, within-host competition causes R_S carriers to transition into S_R carriers over time. However, an alternative model proposes that the minor complement of resistant cells in S_R carriers may be outcompeted within

the host over time, transitioning S_R carriers to S carriers. To verify the robustness of our results against the clearance of resistant cells from S_R carriers, we re-fit the the neutral model with succession to the *S. pneumoniae* / penicillin data set assuming that S_R carriers transition to S carriers at double the rate of the R_S to S_R transition, i.e. $2b$. Adding this transition has a minimal impact on the model fit (**Fig. S12**). The relative likelihood of the model fitted with S_R-to-S clearance is 0.926 compared to the model fitted without S_R-to-S clearance.

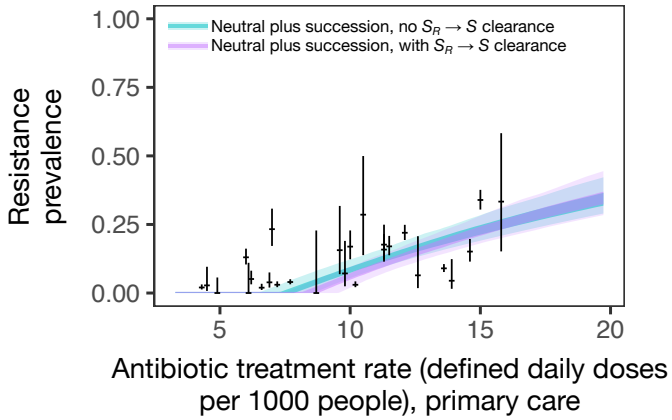

Figure S12 | Model fits for *S. pneumoniae* / penicillin (2007) data set without and with S_R-to-S clearance.

187 **References**

188

189 Apisarnthanarak A, Bailey TC, Fraser VJ. (2008) Duration of stool colonization in
190 patients infected with extended-spectrum β-lactamase-producing *Escherichia*
191 *coli* and *Klebsiella pneumoniae*. *Clin Infect Dis* 46: 1322–1333.
192 Bogaert D, *et al.* (2004) Colonisation by *Streptococcus pneumoniae* and *Staphylococcus*
193 *aureus* in healthy children. *Lancet* 363: 1871–1872.
194 Colijn C, *et al.* (2010) What is the mechanism for persistent coexistence of drug-
195 susceptible and drug-resistant strains of *Streptococcus pneumoniae*? *J. R. Soc.*
196 *Interface* 7: 905–919.
197 European Antimicrobial Resistance Surveillance System (2007) *EARSS Annual Report*
198 *2007*. Bilthoven: EARSS.
199 <https://ecdc.europa.eu/sites/portal/files/media/en/healthtopics/antimicrobi
200 al-resistance-and-consumption/antimicrobial_resistance/publications-
201 documents/Documents/2007_EARSS_Annual_Report.pdf>.
202 European Centre for Disease Prevention and Control (2014) *Surveillance of*
203 *antimicrobial consumption in Europe 2011*. Stockholm: ECDC.
204 <https://ecdc.europa.eu/sites/portal/files/media/en/publications/Publications
205 /antimicrobial-consumption-europe-surveillance-2011.pdf>.
206 European Centre for Disease Prevention and Control (2017a) *Antimicrobial resistance*
207 *surveillance in Europe 2015. Annual Report of the European Antimicrobial*
208 *Resistance Surveillance Network (EARS-Net)*. Stockholm: ECDC.
209 <https://ecdc.europa.eu/sites/portal/files/media/en/publications/Publications
210 /antimicrobial-resistance-europe-2015.pdf>.

211 European Centre for Disease Prevention and Control (2017b) Antimicrobial
212 consumption rates by country.
213 <http://ecdc.europa.eu/en/healthtopics/antimicrobial-resistance-and-
214 consumption/antimicrobial-consumption/esac-net-
215 database/Pages/Antimicrobial-consumption-rates-by-country.aspx>.
216 Larsson AK, *et al.* (2011) Duration of methicillin-resistant *Staphylococcus aureus*
217 colonization after diagnosis: A four-year experience from southern Sweden.
218 *Scand J Inf Dis* 43: 456–462.
219 Lehtinen S, *et al.* (2017) Evolution of antibiotic resistance is linked to any genetic
220 mechanism affecting bacterial duration of carriage. *Proc Natl Acad Sci USA* 114:
221 1075–1080.
222 Li B, *et al.* (2012) Duration of stool colonization in healthy medical students with
223 extended-spectrum-β-lactamase-producing *Escherichia coli*. *Antimicrob Agents*
224 *Chemother* 56: 4558–4559.
225 Martinez-Medina M, *et al.* (2009) Molecular diversity of *Escherichia coli* in the human
226 gut: new ecological evidence supporting the role of adherent-invasive *E. coli*
227 (AIEC) in Crohn's disease. *Inflamm Bowel Dis* 15: 872–882.
228 Shenoy ES, Paras ML, Noubary F, Walensky RP, Hooper DC (2014) Natural history of
229 colonization with methicillin-resistant *Staphylococcus aureus* (MRSA) and
230 vancomycin-resistant *Enterococcus* (VRE): a systematic review. *BMC Infect Dis*
231 14: 177.
232 Ter Braak CJF (2006) A Markov chain Monte Carlo version of the genetic algorithm
233 differential evolution: easy Bayesian computing for real parameter spaces. *Stat*
234 *Comp* 16: 239-249.